Decoupled Beamforming and Noise Cancellation

Jacek P. Dmochowski and Rafik A. Goubran, *Member, IEEE*

***Abstract*—The enhancement of noise-corrupted speech acquired by microphones is indispensable to the functioning of a wide variety of digital signal processing algorithms. Many existing products are equipped with steerable, stand-alone fixed beamformers which provide moderate levels of directivity. Moreover, many applications have long employed the classical adaptive noise canceller configuration with a reference sensor near the noise source to cancel unwanted noise. In this paper, the cascading of stand-alone beamformers with back-end adaptive noise cancellers is studied. A decoupled model for signal enhancement using front-end beamformers and cascaded noise cancellers is presented. The inter-operation of the beamforming and noise canceling units is studied by defining the signal-to-interference ratio (SIR) gain, directivity index, and white noise gain offered by the beamforming and noise cancelling components. The performance of decoupled beamformer-noise canceller structures is evaluated using experimental measurements. An experimental procedure for evaluating output SIR is presented. Results reveal SIR improvements of up to 27 dB, and are compared to those stemming from conventional adaptive beamformers.**

***Index Terms*—Adaptive beamforming, adaptive noise cancellation, delay-and-sum beamformer, generalized sidelobe canceller, microphone arrays.**

I. Introduction

APPLICATIONS requiring the acquisition of far-end speech include stereophonic teleconferencing [1], hands-free communication [2], and human-machine interaction [3]. In these applications, the speech signal is generally contaminated with noise that hinders the proper operation of the involved algorithms. Therefore, there exists a need to remove the presence of the corruptive noise from the received microphone signals.

Arrays of microphones serve as the aperture for digital signal processing algorithms aimed at speech enhancement. A comprehensive review of the state-of-the-art in speech enhancement is given in [4]. It is noted therein that there exists a tradeoff between noise reduction and speech degradation. In other words, in general, the more that one reduces the noise, the more that the speech is distorted. It is important to control this tradeoff to yield the maximal signal-to-noise ratio (SNR).

Classical methods for ridding microphone signals of the effects of noise include adaptive beamforming techniques which minimize total output power subject to a set of linear constraints [5], [6]. Most notably, the minimum variance, distortionless response (MVDR) approach of Capon [7] and its alternative formulation, the Generalized Sidelobe Canceller (GSC) [8], operate with a single constraint and adapt to minimize the power of a given noise field. Sidelobe cancellers exhibit problems when operating in a reverberant environment due to the desired signal cancellation phenomenon. Many solutions to the signal cancellation problem have been proposed; see [9] for a thorough review of these methods.

Several existing products are equipped with steerable, stand-alone fixed beamformers which provide moderate levels of directivity (see [10], for example). Microphone arrays are also sometimes embedded into devices such as micro-electrical-mechanical-systems (MEMS) (see [11]). These are beamformers designed for a specific environment and embedded into a certain shape. Moreover, noise cancelling applications have long employed the classical adaptive noise canceller configuration of [12] with a reference microphone near the noise source to cancel unwanted noise. This paper examines the cascading of stand-alone fixed beamformers with back-end adaptive noise cancellers. The interaction between the front-end beamformers and back-end noise cancellers is examined. An experimental evaluation that measures the signal-to-interference ratio (SIR) gain offered by the respective units is carried out.

It is imperative to understand that the cascading of the beamforming and noise cancelling units is performed without combining the front-end beamforming and subsequent noise cancelling units into a tightly coupled structure. As an example of the latter, the adaptive version of the GSC actually contains front-end beamformers and cascaded adaptive noise cancellers. However, this combination in hardware of beamformers and noise cancellers is *not* the subject of this paper. This paper moves toward a different paradigm for adaptive beamforming in which each component is a stand-alone unit, but may be loosely interconnected with the other to form a "decoupled" structure. The resulting structure is termed the decoupled beamformer-noise canceller (BF-NC).

Section II outlines the signal propagation model used throughout the paper. The decoupled BF-NC model is presented in detail in Section III. The performances of the beamforming and noise cancelling units in a decoupled BF-NC are examined in Section IV. The experimental procedure and results are presented in Section V. Finally, concluding statements are made in Section VI.

II. Signal Model

Consider an array of M microphones and a desired signal source in the far field of the array emitting a signal s. Propagation of the signal to the array is modeled in the time-domain as

$$x_l(n) = \alpha_l s(n - \tau_l) + v_l(n), \quad l = 0, 1, \ldots, M-1 \qquad (1)$$

Manuscript received June 15, 2005; revised October 18, 2006. This paper is based on the Master's thesis work of J. Dmochowski, carried out at the Department of Systems and Computer Engineering, Carleton University, Ottawa, Canada. This work was supported in part by the Ontario Centre of Excellence—Communications and Information Technology Ontario (OCE-CITO), Mitel, Ontario Graduate Scholarships (OGS), and by the National Science and Engineering Research Council of Canada (NSERC).

J. P. Dmochowski is with the INRS-EMT, Université du Québec, Montréal, PQ H5A 1K6, Canada (e-mail: dmochow@emt.inrs.ca).

R. A. Goubran is with the Department of Systems and Computer Engineering, Carleton University, Ottawa, ON K1S 5B6, Canada (e-mail: Rafik.Goubran@sce.carleton.ca).

Digital Object Identifier 10.1109/TIM.2006.887196

where n is the discrete time index, x_l denotes the output of microphone l, τ_l is the propagation delay from the source to microphone l, α_l is an attenuation factor due to propagation effects, and v_l is the additive noise at microphone l and includes any background or sensor noise as well as reverberation. Transposing to the frequency domain and using vector notation, the signal model is compactly written as

$$\mathbf{X}(e^{j\Omega}) = S(e^{j\Omega})\mathbf{d} + \mathbf{V}(e^{j\Omega}) \tag{2}$$

where

$$\mathbf{X}(e^{j\Omega}) = \left[X_0(e^{j\Omega}) \;\; X_1(e^{j\Omega}) \;\; \cdots \;\; X_{M-1}(e^{j\Omega})\right]^T \tag{3}$$

$$\mathbf{V}(e^{j\Omega}) = \left[V_0(e^{j\Omega}) \;\; V_1(e^{j\Omega}) \;\; \cdots \;\; V_{M-1}(e^{j\Omega})\right]^T \tag{4}$$

$$\mathbf{d} = \left[\alpha_0 e^{-j\Omega\tau_0} \;\; \alpha_1 e^{-j\Omega\tau_1} \;\; \cdots \;\; \alpha_{M-1} e^{-j\Omega\tau_{M-1}}\right]^T \tag{5}$$

is the propagation vector, $S(e^{j\Omega})$, $X_l(e^{j\Omega})$, and $V_l(e^{j\Omega})$ denote the discrete-time Fourier transform of $s(n)$, $x_l(n)$, and $v_l(n)$, respectively, ^{T} denotes the transpose of a vector or matrix, and Ω denotes discrete frequency.

The microphones are filtered and then summed across the array to form the beamformer output

$$Z(e^{j\Omega}) = \mathbf{W}^H(e^{j\Omega})\mathbf{X}(e^{j\Omega}) \tag{6}$$

where

$$\mathbf{W}^H(e^{j\Omega}) = \left[W_0^*(e^{j\Omega}) \;\; W_1^*(e^{j\Omega}) \;\; \cdots \;\; W_{M-1}^*(e^{j\Omega})\right] \tag{7}$$

represents the traditional beamformer, ^{H} denotes the conjugate transpose and * the complex conjugate.

III. Decoupled Beamformer-Noise Canceller Model

Fig. 1 exhibits the decoupled BF-NC model. The front-end is composed of a bank of beamformers (denoted in the figure by BF) which may belong to any class of spatial filters: delay-and-sum, filter-and sum, constant-directive [13], etc.

The design of these beamformers is performed *a priori* for a specific environment and the beamformers come equipped with steerable beams. The steering of these beamformers is performed by an intelligent beam-steering module, which operates as a "look-up" table. The control unit scans the environment, determines the locations of the signal and interference sources, and then feeds these locations to the beam-steering module. The beam-steering module then translates these locations to appropriate beamformer coefficients which are then sent to the beamformers.

The beamformers provide signal references that are fed to the switching module, which then appropriately directs these references to the noise canceller unit. The control unit informs the switching module of which beamformer reference is that of the desired signal, and which beamformers are steered to the interference sources. The desired signal reference is fed to the primary (upper) noise canceller input. Interfering signal references are connected to the reference noise canceller inputs. The noise

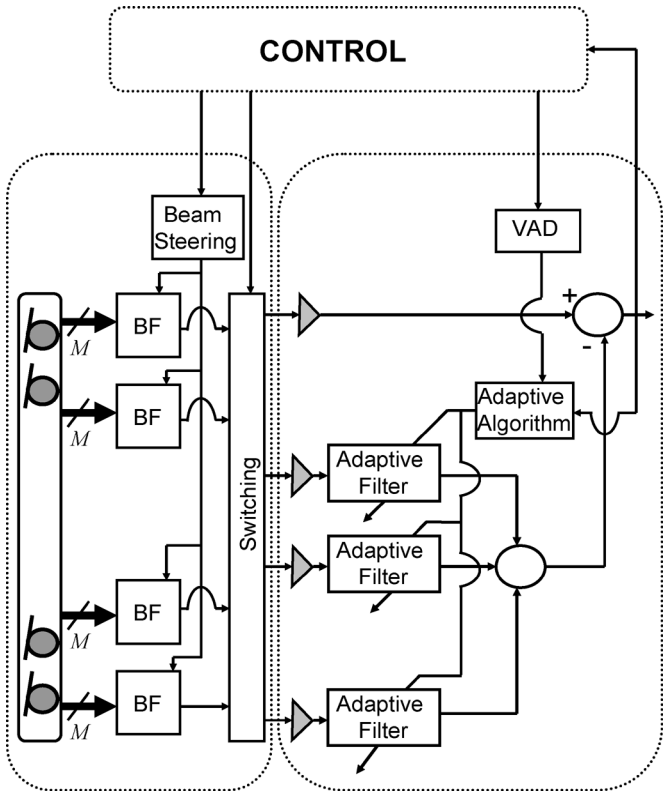

Fig. 1. Structure of a decoupled BF-NC.

cancellers provide added interference attenuation at the directions of arrival (DOA) that correspond to significant interference power. Notice that the noise cancellers are quite separate from the front-end beamformers.

It is important to note that in addition to the decoupled aspect, there is a fundamental difference between this design and that of the GSC. The blocking matrix of the GSC is replaced with fixed beamformers which are steered to the interference sources: instead of steering nulls to the desired signal source, we are steering beams to the interferers. Moreover, in a reverberant environment, these beamformers may also be steered to the significant interfering reflections. The implications of this fundamental change are very important and are discussed thoroughly in future sections.

The decoupled BF-NC scheme is a collection of modules. The emphasis is no longer on optimizing one central beamforming structure, as in the MVDR beamformer. Rather, existing steerable beamformers are loosely connected to a back-end multiple-reference adaptive noise canceller. Beamformers with more "robust" but less directive beams are implemented at the front-end, while significant attenuation of interfering sources is provided by the back-end noise cancellers.

A. Particular Case: Single Interference Source

Assuming a single source of interference, a multiple-reference noise canceller is not needed in the decoupled case, and thus the model of Fig. 1 may be simplified to include only two beamformers and one noise canceller, as shown in Fig. 2. The auxiliary modules have been omitted from the figure. Furthermore, the adaptive filter has been labeled W_{NC}^* which denotes

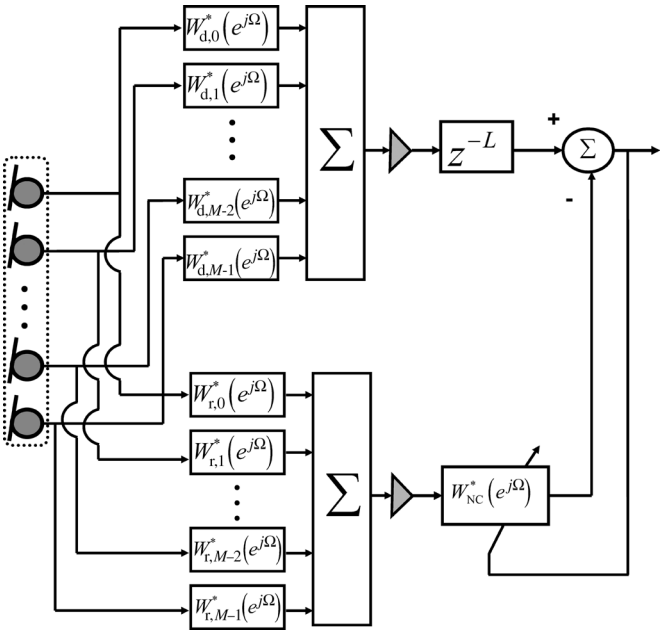

Fig. 2. Decoupled BF-NC with single interference source.

the transfer function of the Wiener solution. A delay of L samples has been included after the desired signal beamformer to ensure causality in the noise canceller transfer function. Each beamformer consists of a bank of finite impulse response (FIR) filters. The beamformer for the desired signal is denoted by

$$\mathbf{W}_d^H(e^{j\Omega}) = \left[W^*_{d,0}(e^{j\Omega})\ W^*_{d,1}(e^{j\Omega})\ \cdots\ W^*_{d,M-1}(e^{j\Omega})\right]. \tag{8}$$

Likewise, the beamformer for the interfering signal, whose output feeds the reference noise canceller input, is

$$\mathbf{W}_r^H(e^{j\Omega}) = \left[W^*_{r,0}(e^{j\Omega})\ W^*_{r,1}(e^{j\Omega})\ \cdots\ W^*_{r,M-1}(e^{j\Omega})\right]. \tag{9}$$

Suppressing the dependence on frequency for brevity, it easily follows that the output of the BF-NC structure is

$$Z = \left(\mathbf{W}_d^H - W^*_{\mathrm{NC}}\mathbf{W}_r^H\right)\mathbf{X}. \tag{10}$$

The power-spectral density (PSD) of the output signal is then

$$\Phi_{\mathrm{ZZ}} = \left(\mathbf{W}_d^H - W^*_{\mathrm{NC}}\mathbf{W}_r^H\right)\mathbf{\Phi}_{\mathrm{XX}}(\mathbf{W}_d - W_{\mathrm{NC}}\mathbf{W}_r) \tag{11}$$

where $\mathbf{\Phi}_{\mathrm{XX}} = E\{\mathbf{X}\mathbf{X}^*\}$ is the cross-spectral density (CSD) matrix of the array input. From [12], the Wiener solution of the noise canceller is given by

$$W_{\mathrm{NC}} = \frac{\mathbf{W}_r^H\mathbf{\Phi}_{\mathrm{XX}}|_{\mathrm{adaptation}}\mathbf{W}_d}{\mathbf{W}_r^H\mathbf{\Phi}_{\mathrm{XX}}|_{\mathrm{adaptation}}\mathbf{W}_r} \tag{12}$$

where $\mathbf{\Phi}_{\mathrm{XX}}|_{\mathrm{adaptation}}$ is the CSD matrix of the array input during the adaptation period. From (10) and (11), it is evident that the decoupled BF-NC structure is effectively an adaptive beamformer with weights given by

$$\mathbf{W}_{\mathrm{effective}} = \mathbf{W}_d - \frac{\mathbf{W}_r^H\mathbf{\Phi}_{\mathrm{XX}}|_{\mathrm{adaptation}}\mathbf{W}_d}{\mathbf{W}_r^H\mathbf{\Phi}_{\mathrm{XX}}|_{\mathrm{adaptation}}\mathbf{W}_r}\mathbf{W}_r. \tag{13}$$

Therefore, the structure of Fig. 2 may be implemented in the canonical beamformer form (i.e., a bank of FIR filters). The notation of (13) simplifies the evaluation of decoupled BF-NC structures. A simple decoupled BF-NC structure with two delay-and-sum beamformers (DSBs) and a single channel noise canceller is presented in [14]. Using the model of Fig. 2, the structure is defined as:

$$\mathbf{W}_d^H = \frac{1}{M}\mathbf{d}_s^H = \frac{1}{M}\left[1\ e^{j\Omega\tau_1^s}\ \cdots\ e^{j\Omega\tau_{M-1}^s}\right] \tag{14}$$

$$\mathbf{W}_r^H = \frac{1}{M}\mathbf{d}_i^H = \frac{1}{M}\left[1\ e^{j\Omega\tau_1^i}\ \cdots\ e^{j\Omega\tau_{M-1}^i}\right] \tag{15}$$

where $\mathbf{d}_s$ and $\mathbf{d}_i$ are the propagation vectors of the signal and interference, respectively, τ_k^s is the relative propagation delay between microphones 0 and k for the desired signal source, and τ_k^i is the relative propagation delay between microphones 0 and k for the interference source. In other words, the upper beamformer is a DSB steered to the signal source, while the lower beamformer is a DSB steered to the interference. Using (12), and assuming that the adaptation is performed with only the interference source active, the Wiener solution of this structure is easily found to be

$$W_{\mathrm{NC}} = \frac{1}{M}\mathbf{d}_i^H\mathbf{d}_s. \tag{16}$$

Therefore, for this structure

$$\mathbf{W}_{\mathrm{effective}} = \frac{1}{M}\mathbf{d}_s - \frac{1}{M^2}\mathbf{d}_i^H\mathbf{d}_s\mathbf{d}_i. \tag{17}$$

One advantage of employing such a structure is the reduced complexity: only a single adaptive filter is needed. Furthermore, note that the desired signal cancellation phenomenon that occurs as a result of the sensitivity of the blocking matrix is averted, as one is no longer steering the reference beamformer to the desired signal. The key to avoiding signal cancellation is to minimize the SIR at the reference noise canceller input(s) [12]. In the decoupled BF-NC, if the steering direction of the interference is misjudged, the SIR at the adaptive filter input will increase by an amount proportional to the slope of the interference beam's main lobe. Conversely, in the GSC, a steering error leads to a SIR increase proportional to the slope of the null of the blocking matrix. Nulls are steeper than beams, and therefore, the error is expected to be more costly in the GSC.

The structure in Fig. 2 is applicable to environments with a single interference source. The structure may easily be generalized to an arbitrary number of interferers by adding a lower branch for every additional source of interference. Each additional branch consists of a DSB steered to the corresponding interference source, and an adaptive filter to remove this interference from the primary input.

IV. Relationships Between Beamforming and Noise Cancellation

It is instructive to analyze the relationship between the beamforming and noise cancelling units of decoupled BF-NC structures. To that end, note that the output SIR may be computed for only the desired-signal beamformer, prior to the noise canceller:

$$\mathrm{SIR}_{\mathrm{BF}} = \frac{\mathbf{W}_d^H \mathbf{\Phi}_{\mathrm{XX}}|_{\mathrm{signal}} \mathbf{W}_d}{\mathbf{W}_d^H \mathbf{\Phi}_{\mathrm{XX}}|_{\mathrm{interference}} \mathbf{W}_d} \tag{18}$$

where $\mathbf{\Phi}_{\mathrm{XX}}|_{\mathrm{signal}}$ is the signal component of the array CSD matrix and $\mathbf{\Phi}_{\mathrm{XX}}|_{\mathrm{interference}}$ is the interference component of the CSD matrix, and the signal and interference are assumed to be temporally uncorrelated. The SIR gain of the front-end beamformer is, thus

$$\mathrm{G}_{\mathrm{BF}}^{\mathrm{SIR}} = \mathrm{SIR}_{\mathrm{BF}} - \mathrm{SIR}_{\mathrm{array}} \tag{19}$$

where $\mathrm{SIR}_{\mathrm{array}}$ is the SIR at the array.

The output SIR produced by the overall BF-NC structure is

$$\mathrm{SIR}_{\mathrm{BF-NC}} = \frac{\mathbf{W}_{\mathrm{effective}}^H \mathbf{\Phi}_{\mathrm{XX}}|_{\mathrm{signal}} \mathbf{W}_{\mathrm{effective}}}{\mathbf{W}_{\mathrm{effective}}^H \mathbf{\Phi}_{\mathrm{XX}}|_{\mathrm{interference}} \mathbf{W}_{\mathrm{effective}}}. \tag{20}$$

It easily follows that the SIR gain of the noise canceller is

$$\mathrm{G}_{\mathrm{NC}}^{\mathrm{SIR}} = \mathrm{SIR}_{\mathrm{BF-NC}} - \mathrm{SIR}_{\mathrm{BF}} \tag{21}$$

while the SIR gain of the decoupled BF-NC is

$$\mathrm{G}_{\mathrm{BF-NC}}^{\mathrm{SIR}} = \mathrm{SIR}_{\mathrm{BF-NC}} - \mathrm{SIR}_{\mathrm{array}}. \tag{22}$$

We may do the same for the directivity index (DI). The directivity offered by the front-end beamformer alone is given by

$$DI_{\mathrm{BF}} = \frac{\left|\mathbf{W}_d^H \mathbf{d}_s\right|^2}{\mathbf{W}_d^H \mathbf{\Gamma}_{\mathrm{nn}}|_{\mathrm{diffuse}} \mathbf{W}_d} \tag{23}$$

where $\mathbf{\Gamma}_{\mathrm{nn}}|_{\mathrm{diffuse}}$ is the coherence matrix of a diffuse noise field.

The DI of the decoupled BF-NC is

$$DI_{\mathrm{BF-NC}} = \frac{\left|\mathbf{W}_{\mathrm{effective}}^H \mathbf{d}_s\right|^2}{\mathbf{W}_{\mathrm{effective}}^H \mathbf{\Gamma}_{\mathrm{nn}}|_{\mathrm{diffuse}} \mathbf{W}_{\mathrm{effective}}}. \tag{24}$$

Finally, the white noise gain (WNG) offered by the front-end beamformer is

$$WNG_{\mathrm{BF}} = \frac{\left|\mathbf{W}_d^H \mathbf{d}_s\right|^2}{\mathbf{W}_d^H \mathbf{W}_d} \tag{25}$$

while the WNG of the decoupled BF-NC is

$$WNG_{\mathrm{BF-NC}} = \frac{\left|\mathbf{W}_{\mathrm{effective}}^H \mathbf{d}_s\right|^2}{\mathbf{W}_{\mathrm{effective}}^H \mathbf{W}_{\mathrm{effective}}}. \tag{26}$$

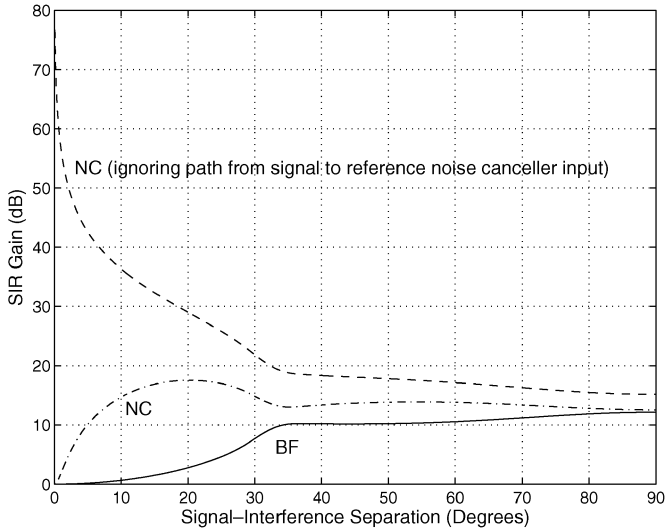

Fig. 3. SIR relationships between beamformer and noise canceller.

Examination of the relationships between the quantities (19) and (21), (23) and (24), and (25) and (26) sheds light into the interoperation of the beamforming and noise cancelling components.

The SIR gains of the beamforming and noise cancelling units have been determined for various signal-interference spatial separations. The decoupled structure defined by (14) and (15) is assumed to compute the SIR gains. An $M = 4$ element, uniformly-spaced, linear array with an inter-element spacing of 0.046 m is assumed. The desired signal source is located at broadside. Both the signal and interference are assumed to be white with a unit PSD across the frequency range of interest. There is a perfect correspondence between array steering and the signals' directions of arrival (DOA). A spatially uncorrelated Gaussian noise field with a SNR of 20 dB is assumed. The sampling frequency is 8 kHz, and the results are averaged over the 300 Hz–3.7 kHz frequency band. Adaptation is performed in the absence of the desired signal. Fig. 3 shows the SIR relationships. For the SIR gain of the noise canceller, two curves are shown: one curve taking into account the presence of desired signal components in the reference noise canceller input, and the other ignoring this presence (a rather artificial curve). In the figure, BF refers to beamformer and NC to the noise canceller.

The curve clearly illustrates the opposing nature of the BF and NC units. While the SIR gain of the beamformer increases with increased signal-interference separation, the SIR gain of the noise canceller generally decreases with increased separation. A beamformer is a structure that thrives on spatial separation between desired signal and interference sources. Since the amount of interference leaked through the desired signal beamformer decreases as the interference source moves away from the signal look-direction, the SIR at the desired signal beamformer output increases for increased signal-interference separation. On the other hand, a noise canceller is a purely temporal device that relies on correlation between its primary and reference inputs to convert the adaptive filter input to the desired signal. Intuitively, the correlation between beamformer outputs decreases as the steering directions of the beamformers move

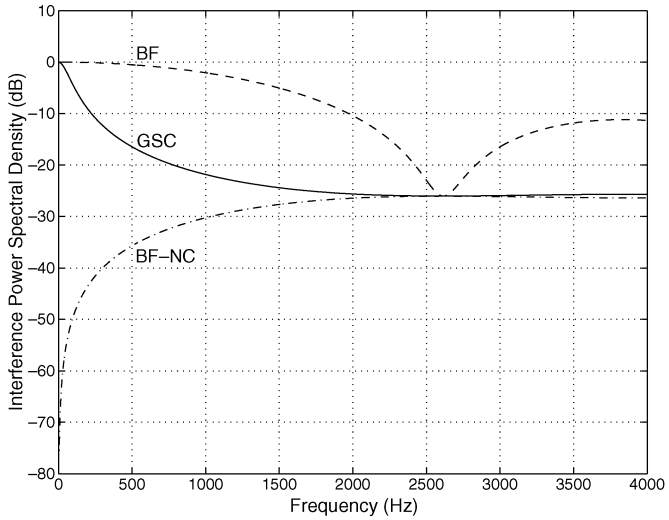

Fig. 4. Interference power levels as a function of frequency.

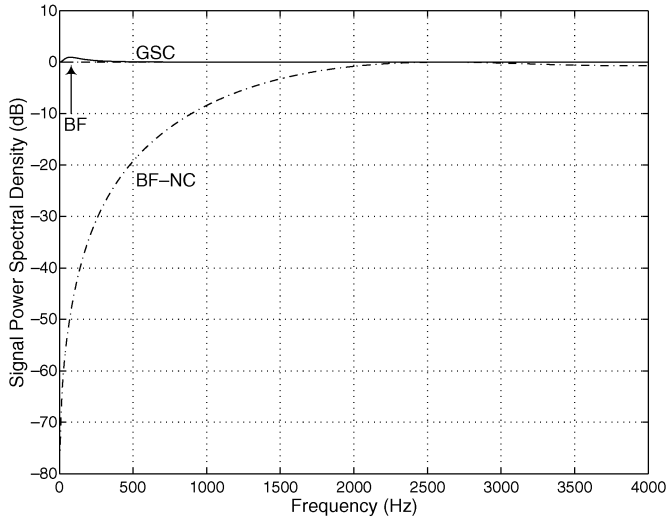

Fig. 5. Signal power levels as a function of frequency.

away from each other. Formally, note that the level of interference reduction in the noise canceller is related to the interference-to-uncorrelated-noise ratio (IUNR) at the primary input, according to [12]. As the interference source moves away from the desired signal look direction, the level of interference at the primary noise canceller input decreases. However, the level of uncorrelated noise at the primary noise canceller input obviously does not depend on the position of the interference, and thus the IUNR decreases with increased signal-interference separation. Consequently, the SIR gain of the noise canceller decreases as the signal-interference separation increases. Notice that when taking into account the path from signal to reference noise canceller input, for small signal-interference separation (i.e., 0°–20°), the noise canceller suffers from a large amount of leakage of the desired signal into its reference input, according to [12]. This occurs because the steering directions of the two beamformers are similar. As a result, the desired signal is passed through the interference beam, and signal distortion occurs.

To examine the frequency-dependent nature of the SIR gains produced by the components of the decoupled BF-NC, the PSDs of the interference and signal are computed for a signal-interference separation of 45°. In order to compare the performance of the decoupled BF-NC to that of a standard adaptive beamformer, the frequency-dependent SIR gain of the GSC is also computed.

Fig. 4 shows the interference power levels as a function of frequency at the front-end beamformer output, decoupled BF-NC output, and GSC output. (The signal and interference PSD at the array is 0 dB for all frequencies.) It is clear that the greatest interference cancellation is provided by the decoupled BF-NC. It is well known [15] that the level of noise reduction offered by an adaptive noise canceller is intimately related to the coherence between the primary and reference noise canceller inputs. The decoupled BF-NC minimizes the level of uncorrelated noise in the reference noise canceller input, and thus maximizes the coherence between primary and noise canceller inputs, leading to a low minimum-mean-squared-error (mmse) in the adaptation process. In the GSC, the reference beamformer is the blocking matrix, which does not provide the same level of sensor noise suppression as a DSB. Moreover, the level of interference in the blocking matrix outputs is lower than that of the reference beamformer output of the decoupled BF-NC. The coherence between primary and reference inputs in the GSC is less than in that of the decoupled structure, leading to a higher mmse. Therefore, the level of interference cancellation is not as great. The beamformer alone generally provides only moderate levels of interference reduction. Note that the dip in the front-end beamformer curve at 2600 Hz is due to a null in the beamformer's beampattern at that frequency in the direction of the interference.

Fig. 5 displays the frequency-dependent desired signal power levels. The disadvantage of the decoupled BF-NC is shown in the form of desired signal distortion at the low frequency end. This is a direct result of the desired signal being passed through the sidelobes of the interference beamformer. The blocking matrix prevents any such leakage, and, thus, the GSC preserves the desired signal power levels at the array. The stand-alone beamformer also maintains the signal power. From Figs. 4 and 5, the tradeoff between noise reduction and signal distortion is evident. The decoupled structure maximizes the noise coherence between the primary and reference noise canceller inputs; however, in order to provide this raised level of coherence, leakage of the signal into the reference noise canceller input results.

Fig. 6 displays the overall SIR gains provided by the front-end beamformer, decoupled BF-NC, and GSC. It is somewhat surprising that the decoupled BF-NC and GSC actually provide equivalent levels of SIR gain across all frequencies, especially considering the curves of Figs. 4 and 5. The manners in which the decoupled BF-NC and GSC accomplish this SIR gain are quite different, but the end result is the same. Note that the complexity of the decoupled BF-NC is significantly lower than that of the GSC. The spike in the front-end beamformer curve corresponds to a null in the beampattern in the direction of the interferer at that frequency.

The effect of including the noise canceller on the DI of the decoupled BF-NC is evaluated using (23) and (24). The parameters used are the same as those used to compute the SIR gains, with the exception that for the decoupled BF-NC, the desired

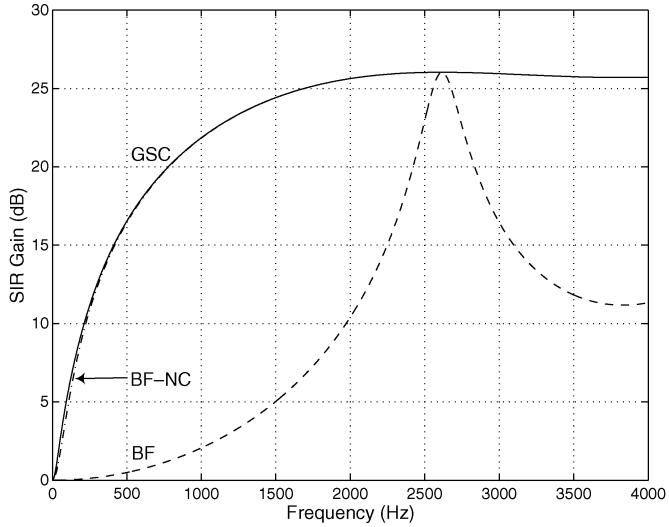

Fig. 6. SIR gain as a function of frequency.

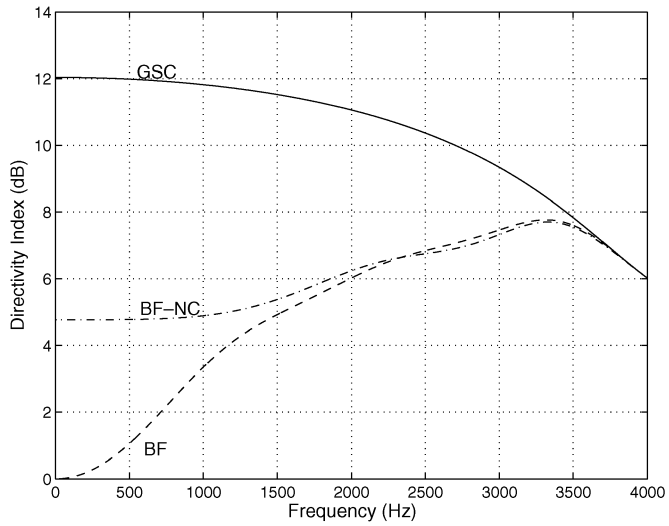

Fig. 7. Directivities of beamformer, decoupled BF-NC, and GSC.

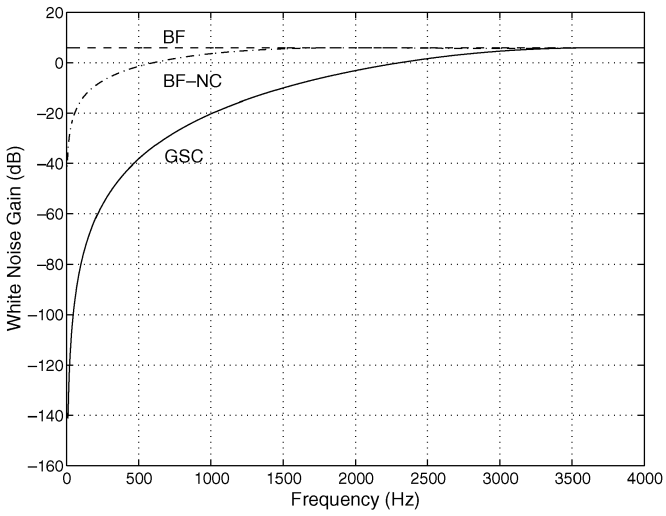

Fig. 8. White noise gains of beamformer, decoupled BF-NC, and GSC.

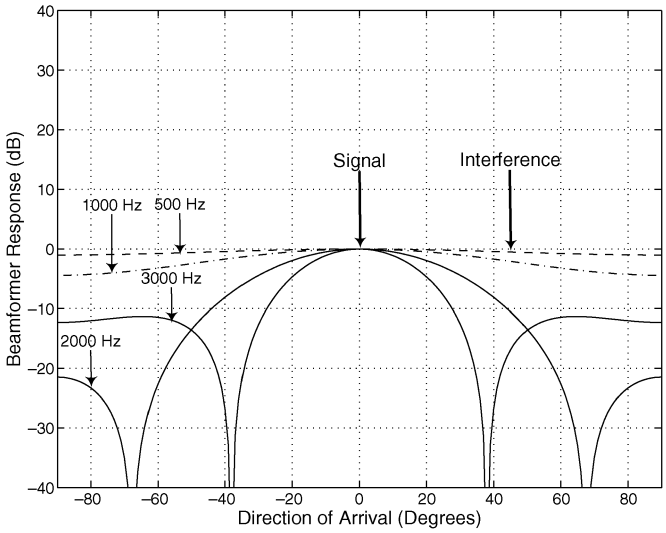

Fig. 9. Beam patterns of front-end beamformer for various frequencies.

signal DSB is steered to the endfire direction, while the interference DSB is steered to broadside. The DI of the GSC is also computed—for the computation, both the desired signal beamformer and blocking matrix are steered to the endfire direction. Fig. 7 displays the DI of the front-end beamformer, the decoupled BF-NC structure, and the GSC.

The decoupled BF-NC structure enhances the directivity over the DSB only in the lower frequency range. This is because a single reference beamformer is limited in its ability to "capture" the noise field. The single noise canceller is more suited to removing a spatially colored noise field (i.e., an interferer) as opposed to a diffuse noise field. On the other hand, the multiple-output blocking matrix of the GSC better captures the diffuse field, and the resulting multiple-reference noise canceller provides more attenuation. The GSC is the optimal beamformer in terms of maximizing the DI.

The effect of cascading the beamformer with the noise canceller on the WNG of the decoupled BF-NC is evaluated using (25) and (26). The same parameters as those used to compute the DI are used. Fig. 8 depicts the WNG of the front-end beamformer, the decoupled BF-NC, and the GSC.

It is not surprising that the addition of the noise canceller in the decoupled structure reduces the WNG—the DSB at the front-end is the optimal beamformer for maximizing the WNG. The degradation is most noticeable at the low end of the frequency spectrum, as the transfer function of the converged adaptive filter is low pass [16]. In the GSC, the presence of the blocking matrix and ensuing multiple-channel noise canceller further degrades the WNG. This is because there are now $M-1$ adaptive filters, each of which augments the uncorrelated noise at the output. The noise canceller is unable to cancel any uncorrelated noise components in its inputs, and thus the degradation of Fig. 8 ensues.

Finally, the beampatterns of the front-end beamformer, decoupled BF-NC, and GSC structures (all steered to broadside) have been computed. The computation uses the same $M = 4$ element array; during the adaptation, only the interference source is active and impinges on the array at a DOA of 45°.

From Fig. 9, the front-end beamformer provides very low levels of directivity at the lower frequency end; at the higher frequencies, the locations of the beamformer nulls vary with frequency. It is evident from Fig. 10 that the addition of the noise

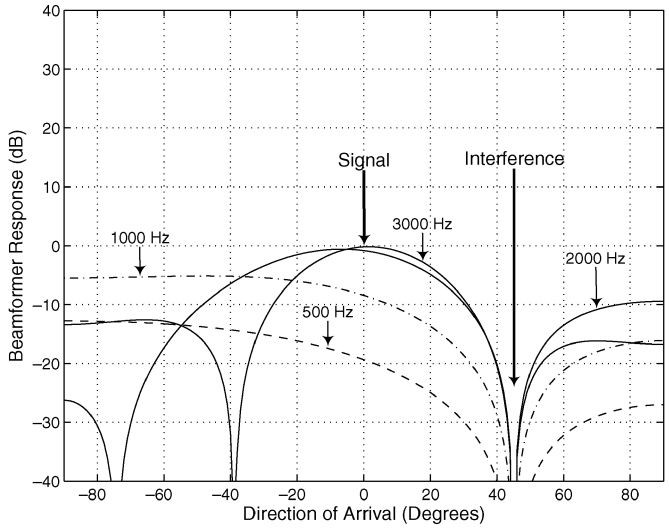

Fig. 10. Beam patterns of decoupled BF-NC for various frequencies.

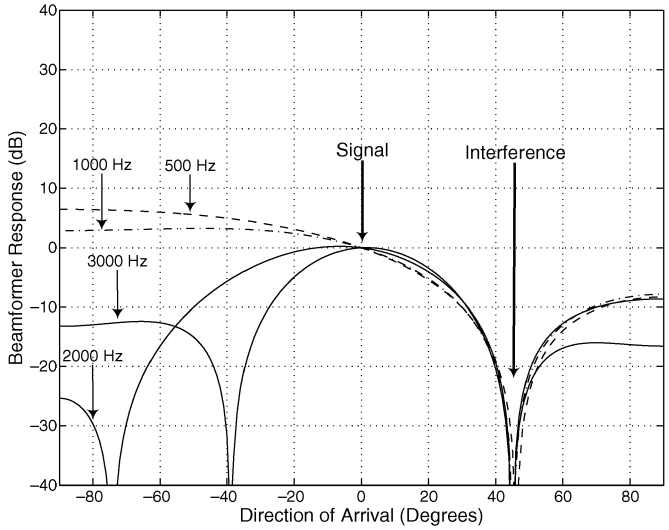

Fig. 11. Beam patterns of GSC for various frequencies.

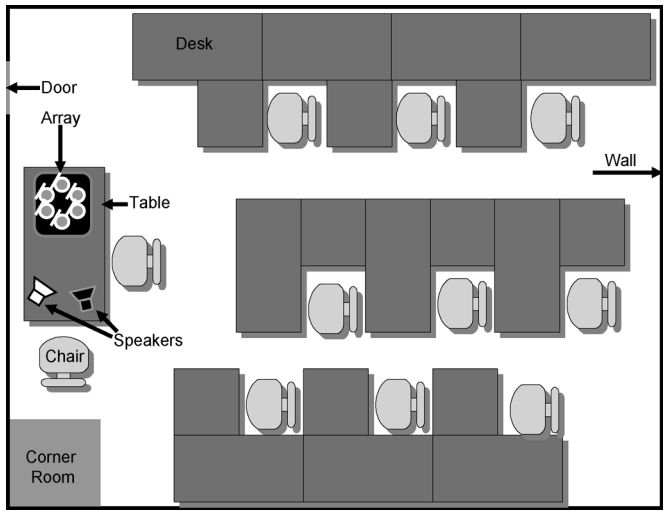

Fig. 12. Layout of room used in experiment.

canceller forces a null in the direction of the interference at all frequencies. However, some signal attenuation also occurs at the lower frequencies. Nevertheless, even at these frequencies, the SIR is still high due to the depth of the interference null. From Fig. 11, the constraint forces a unity gain response of the GSC in the direction of the signal, while forming deep nulls in the direction of the interference. The price paid for this is the inclusion of $M-2$ additional adaptive noise cancellers.

A number of researchers have investigated beamformers from an experimental point-of-view [17]–[19]. The next section details an experimental evaluation of decoupled BF-NC structures.

V. Evaluation in a Real Environment

An experimental evaluation of the decoupled BF-NC defined by (14) and (15) is performed. The performance of the GSC is also evaluated for comparison purposes. The experiments are performed in a large office-room, whose layout is shown in Fig. 12. The room dimensions are 11 m by 9.5 m by 3 m. The data acquisition unit consists of a circular, sector-based, six-element microphone array with a 5 cm radius, a preamplifier, a multichannel computer sound card, and recording software. The sound sources are ordinary personal computer speakers. The sampling rate of the sound card is chosen to be 8 kHz, with a 16-bit analog-to-digital conversion. The specifications of the data acquisition unit are given in Table I.

Throughout the experiment, the sound sources and microphone array rest on a wooden table. The microphone array is not calibrated. Both desired and interfering signals are chosen to be independent realizations of a band-limited (300 Hz–3.7 kHz) white Gaussian process. The subsequent signal processing is performed offline in the MATLAB environment. In order to compute the optimal delays to perform delay-and-sum beamforming at the front-end, the generalized cross-correlation method [20] for time delay estimation with no frequency weighting is employed. A delay of $L = 100$ samples is implemented at the desired signal beamformer output for causality. The normalized least-mean-square (NLMS) algorithm with a step-size of $\alpha = 0.1$ is employed, with the adaptive filters having lengths of 200 taps. The adaptation is performed with only the interference source playing.

Throughout the evaluation, the location of the interference source is held fixed, while the desired signal source is moved around to various locations, as shown in Fig. 13. The objective of the evaluation is to determine the improvement in SIR from signal acquisition point (microphone array) to system output point for each signal-interference spatial configuration. It is important to note that since the investigation employs real (as opposed to simulated) data, the evaluation cannot be performed with desired signal and interference playing simultaneously. The experimental procedure consists of two stages. In the first stage, only the interference is captured with the array, and beamformed accordingly. The adaptive algorithm then computes the optimal transfer function between the two beamformer outputs. The captured interference is then fed back into the converged structure, and the output interference power is measured. In the second stage, the desired signal (and only the desired signal) is recorded with the array and subsequent components. The recorded signal is then applied to the converged

TABLE I
SPECIFICATIONS OF DATA ACQUISITION UNIT

Component	Specifications
Microphone array	6-element equispaced circular array with 10 cm diameter, electret condenser mics
Pre-amplifier	proprietary Mitel
Multi-channel sound card	M-Audio Delta 1010
Recording software	Adobe Audition, version 7.0
Personal computer	Dell Dimension DIM6400, Pentium 4 CPU, 2.80 GHz
Audio playback software	Microsoft Windows Media Player, version 9.00.003250
PC loudspeaker	harman/kardon multimedia speaker system

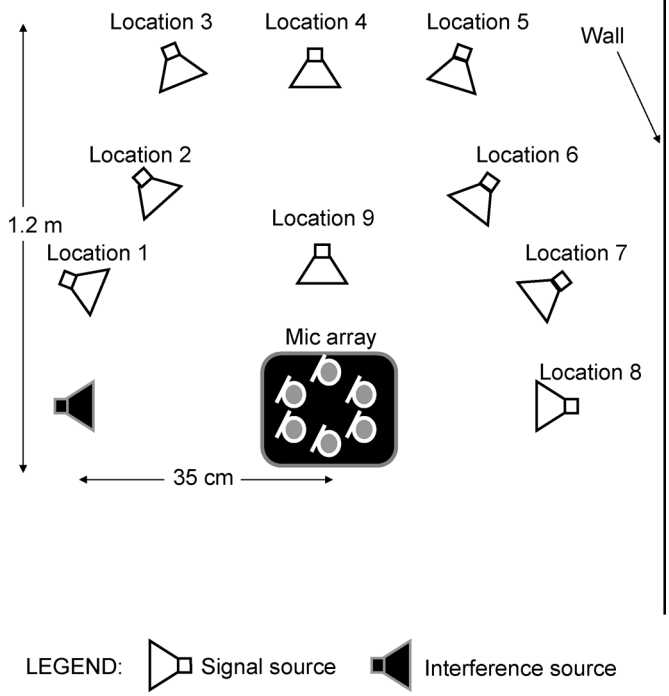

Fig. 13. Signal-interference configurations in experiment.

structure being evaluated, and once again, the output signal power is recorded. The output SIR is then easily determined by combining the results of the two stages. Note that since the system is linear, the latter procedure is valid. Table II depicts the SIR improvements offered by the front-end beamformer, the decoupled BF-NC structure, and the GSC.

The sensitivity of the front-end beamformer to the location of the desired signal source is evident from Table II. In particular, when the signal source is located near the wall, the desired signal beam strongly picks up interfering signal reflections. This is evidenced from the low beamformer SIR gains experienced when the desired signal source rests near the wall. However, it is apparent that a low SIR gain at the front-end beamformer does not translate to reduced noise canceller SIR gain. The noise canceller is able to "compensate" for the lowered directivity of the beamformer. Note that the noise cancellers are adapted in the presence of reverberation, and thus, the filter taps will be driven

TABLE II
MEASURED SIR GAINS (dB) OF FRONT-END BEAMFORMER (**BF**), DECOUPLED BEAMFORMER-NOISE CANCELLER (**BF-NC**), AND GENERALIZED SIDELOBE CANCELLER (**GSC**)

Location	**BF**	**BF-NC**	**GSC**
1	2.92	26.10	28.14
2	9.24	27.16	27.22
3	8.61	24.43	25.30
4	7.04	25.01	25.56
5	4.13	25.96	25.15
6	4.24	26.54	25.31
7	2.15	26.66	25.47
8	4.48	26.48	26.99
9	5.12	25.38	26.69

to cancel any interference reflections in the desired signal beamformer output. Because the adaptation is carried out in the absence of the desired signal, cancellation of the desired signal due to signal reflections does not result. Even though reverberation does lead to the leakage of the desired signal into the reference noise canceller input, the filter is no longer being adapted, and thus only a distortion of the signal occurs.

Notice that there is only one location at which the GSC significantly outperforms (i.e., by $\sim$2 dB) the decoupled structure, and that this location corresponds to the smallest signal-interference separation. At this location, the signal leakage into the reference noise canceller input(s) becomes the dominant factor. The GSC's blocking matrix forms a null in the direction of the desired signal source, thus lowering the level of signal distortion. On the other hand, at all other locations, the decoupled BF-NC structure provides either superior or equivalent performance as that of the GSC. Note that the decoupled structure requires $M-2$ less adaptive filters. The improved noise coherence between the primary and reference noise canceller inputs offered by the decoupled structure leads to this good performance despite the lowered complexity. Thus, even though the decoupled BF-NC allows more signal leakage into the reference noise canceller inputs than the GSC, the increased level of interference reduction provided by the BF-NC leads to an equivalent or superior SIR than that of the GSC.

VI. Conclusion

This paper has presented a decoupled-model for signal enhancement which intelligently cascades existing front-end fixed beamformers with adaptive noise cancellers.

It was shown that decoupled BF-NC structures provide increased noise coherence between the primary and reference noise canceller inputs over conventional adaptive beamformers. On the other hand, decoupled structures result in some signal leakage into the reference noise canceller input(s). A tradeoff between noise reduction and desired signal distortion ensues.

An experimental procedure for measuring SIR gain was presented, and experimental results showed that it is possible to achieve SIR gains as high as 27 dB with a simple decoupled structure with only two DSBs and a single-channel adaptive noise canceller. Instead of blocking the desired signal with a multiple-input-multiple-output blocking matrix, such decoupled structures attempt to minimize the SIR at the reference noise canceller input(s) by steering a beam to the interference.

Acknowledgment

The authors would like to thank Dr. F. Beaucoup at Mitel for contributing several valuable discussions that helped improve the quality of this paper.

References

[1] M. M. Sondhi and D. R. Morgan, "Acoustic echo cancellation for stereophonic teleconferencing," in *Proc. 1991 IEEE ASSP Workshop on Appls. Signal Processing Audio and Acoustics*, 1991, pp. 141–142.

[2] G. Lathoud, J. Bourgeois, and J. Freudenberger, "Sector-based detection for hands-free speech enhancement in cars," *EURASIP J. Appl. Signal Process.*, vol. 2006, 2006, Article ID 20683, 15 pp..

[3] D. O'Shaughnessy, *Speech Communications: Human and Machine*, 2nd ed. New York: IEEE, 2000.

[4] J. Benesty, S. Makino, and J. Chen, Eds., *Speech Enhancement*. Berlin, Germany: Springer, 2005.

[5] O. L. Frost, "An algorithm for linearly constrained adaptive array processing," *Proc. IEEE*, vol. 60, pp. 926–935, Aug. 1972.

[6] B. D. Van Veen and K. M. Buckley, "Beamforming: a versatile approach to spatial filtering," *IEEE ASSP Mag.*, vol. 5, pp. 4–24, Apr. 1988.

[7] J. Capon, "High-resolution frequency-wavenumber spectrum analysis," *Proc. IEEE*, vol. 57, pp. 1408–1418, Aug. 1969.

[8] L. J. Griffiths and C. W. Jim, "An alternative approach to linearly constrained adaptive beamforming," *IEEE Trans. Antennas Propag.*, vol. AP-30, pp. 27–34, Jan. 1982.

[9] O. Hoshuyama and A. Sugiyama, "Robust adaptive beamforming," in *Microphone Arrays: Signal Processing Techniques and Applications*, M. S. Brandstein and D. B. Ward, Eds. Berlin, Germany: Springer-Verlag, 2001, pp. 87–109.

[10] F. Beaucoup, "Parallel beamformer design under response equalization constraints," in *Proc. IEEE Int. Conf. Acoust., Speech, Signal Process.*, 2004, vol. 5, pp. II-205–II-208.

[11] S. Chowdhury, M. Ahmadi, and W. C. Miller, "Design of a MEMS acoustical beamforming sensor microarray," *IEEE Sens. J.*, vol. 2, pp. 617–627, Dec. 2002.

[12] B. Widrow *et al.*, "Adaptive noise cancelling: principles and applications," *Proc. IEEE*, vol. 63, pp. 1692–1716, 1975.

[13] D. B. Ward, R. A. Williamson, and R. C. Williamson, "FIR filter design for frequency-invariant beamformers," *IEEE Signal Process. Lett.*, vol. 3, no. 3, pp. 69–71, Mar. 1996.

[14] J. Dmochowski and R. A. Goubran, "Noise cancellation using fixed beamforming," in *Proc. IEEE Int. Workshop on Haptic, Audio, and Visual Environments and their Applicat. (HAVE)*, Oct. 2004, pp. 141–145.

[15] J. J. Rodriguez, Adaptive Noise Reduction in Aircraft Communication Systems MIT Lincoln Lab., Lexington, MA, Tech. Rep. 756, Jan. 1987.

[16] J. Dmochowski, "Combined beamforming and noise cancellation," M.A. Sc. degree thesis, Carleton Univ., Ottawa, ON, Canada, 2003–2005.

[17] Y. R. Zheng, R. A. Goubran, and M. El-Tanany, "Experimental evaluation of a nested microphone array with adaptive noise cancellers," *IEEE Trans. Instrum. Meas.*, vol. 53, pp. 777–786, Jun. 2004.

[18] E. M. Petriu, N. D. Georgonas, D. C. Petriu, D. Makrakis, and V. Z. Groza, "Sensor-based information appliances," *IEEE Instrum. Meas. Mag.*, vol. 3, pp. 31–35, Dec. 2000.

[19] J. Huang, N. Ohnishi, and N. Sugie, "Sound localization in reverberant environment based on the model of the precedence effect," *IEEE Trans. Instrum. Meas.*, vol. 36, pp. 842–846, Aug. 1997.

[20] C. H. Knapp and G. C. Carter, "The generalized correlation method for estimation of time delay," *IEEE Trans. Acoust. Speech Signal Process.*, vol. 24, pp. 320–327, Aug. 1976.

Jacek P. Dmochowski was born in Gdansk, Poland, in December 1979. He received the Bachelor of Engineering degree with High Distinction in communications engineering and the Master's degree of applied science in electrical engineering from Carleton University, Ottawa, Canada, in 2003 and 2005, respectively. He is currently pursuing the Ph.D. degree at the Université du Québec, INRS-EMT, Montréal, QC, Canada.

His research interests include microphone array beamforming and source localization, as well as frequency-domain uncertainty analysis.

Rafik A. Goubran (M'87) received the B.Sc. and M.Sc. degrees in electrical engineering from Cairo University, Cairo, Egypt, in 1978 and 1981, respectively. He received the Ph.D. degree in electrical engineering from Carleton University, Ottawa, ON, Canada, in 1986.

In January 1987, he joined the Department of Systems and Computer Engineering, Carleton University, where he is now a Professor. He is presently Acting Dean of the Faculty of Engineering and Design at Carleton University. He was involved in several research projects with industry and government organizations. His research interests include digital signal processing and instrumentation and their applications in audio processing and biomedical engineering, VoIP, noise and echo cancellation, and beamforming using microphone arrays.

Dr. Goubran is a member of the Association of Professional Engineers of Ontario.